IRAM - 282

The gas component in galaxies: Atomic and molecular gas Distributions

Sept 1992

M. Guélin

IRAM, St Martin d'Heres

IRAM N°282

2nd Course: CURRENT TOPICS IN ASTROFUNDAMENTAL PHYSICS
ETTORE MAJORANA CENTRE FOR SCIENTIFIC CULTURE
INTERNATIONAL SCHOOL OF ASTROPHYSICS D. CHALONGE

Erice - Sicily : 6 – 13 September 1992

THE GAS COMPONENT IN GALAXIES: ATOMIC AND MOLECULAR GAS DISTRIBUTIONS

M. GUÉLIN
IRAM, 300 rue de la piscine, 38406 St-Martin-D'Heres, France

ABSTRACT.
The molecular gas distribution in the Milky Way and in external galaxies is usually derived by assuming the H_2 column density is simply proportional to the CO 2.6 mm line intensity. The observational support (and possible theoretical justification) for the existence of such a relation in the Galaxy will be discussed. Arguments will be presented on whether this 'standard' factor also applies to other galaxies. Finally, the distributions of the molecular gas in our Galaxy and in a few other systems, derived either from the 'standard' factor methods, or from alternative methods, will be presented and compared with the distributions of HI and of the stars.

Introduction

The interstellar (IS) gas, whose importance has been recognized only in the late 1920s, plays a fundamental role in the evolution of galaxies. For long, this gas was thought to be mostly in the form of HI atoms. The 21 cm HI line provided then a simple way to study its mass distribution (and dynamics) in the Milky Way and in the closest galaxies.

Since twenty years, we know that IS hydrogen is at least as much in the form of molecules as in the form of atoms; the 21 cm HI maps of the Galaxy (and of external systems) yield thus an incomplete picture of this gas. Unfortunately, even from space, the H_2 molecule is difficult to detect outside the lines of sight to excited regions and bright stars. The study of the molecular gas has to rely on the observation of minor constituants, primarily CO.

CO is readily detectable at millimeter wavelenghts through its lowest rotation lines at 2.6 mm, 1.3 mm, 0.86 mm wavelength. The brightness of the $^{12}C^{16}O$ lines is high (few kelvin) and the large antennas and interferometers provide few arc-second resolutions at those wavelengths –high enough to allow detailed studies of some galaxies. The $^{12}C^{16}O$ lines, however, are optically thick, making the derivation of the CO column densities difficult. The lines of the rare isotopomers, $^{13}C^{16}O$ and $^{12}C^{18}O$, are weak and easily observable only in the vicinity of the sun. Moreover, the CO to H_2 abundance ratio, few $\times 10^{-4}$ at most, is highly variable, making the conversion of CO line intensities into H_2 masses uncertain.

The opacity of the CO lines and the variability of the CO/H_2 ratio has not prevented radio astronomers to use extensively CO as a tracer of H_2 and to infer the molecular gas column density from the intensity of its millimetre lines. The trick lies in an empirically derived 'conversion' factor which seems to rely the $^{12}C^{16}O$ line velocity-integrated intensity, W(CO), to the H_2 column density, $N(H_2)$. By assuming this factor applies universally, the molecular mass distributions in the Galaxy and in number of external systems have been derived.

The Distant Ultraluminous Object IRAS10214+4724

One of the most impressive results of the last two years in extragalactic astronomy has been the measure of the redshift of the IR-bright galaxy 10214+4724 (Rowan-Robinson et al. 1991). This seemingly faint IRAS source was identified with a galaxy with a redshift z= 2.286 and became one of the most luminous objects in the Universe. It was subsequently detected in the J=3–2 through 6–5 lines of $^{12}C^{16}O$ (Brown and Vanden Bout 1991, Solomon et al. 1992 – see Fig. 1).

The CO observations provided a high resolution spectrum of 10214+4724, hence detailed kinematic data (Fig. 1). The moderate width of the line profile implies that the mass of this extraordinary object is probably similar to or smaller than the mass of the large nearby galaxies (otherwise 10214 must be flat and seen face-on). The profile tells us also that this 'primordial' galaxy was already rich in C and O elements as well as in molecular gas.

Using the 'standard Galactic' $N(H_2)/W(CO)$ conversion factor, Solomon and co-authors derived from z and from the integral of the CO profile a H_2 mass $M(H_2)$ of $10^{11} M_\odot$, about 100 times larger than the mass of the Milky Way.

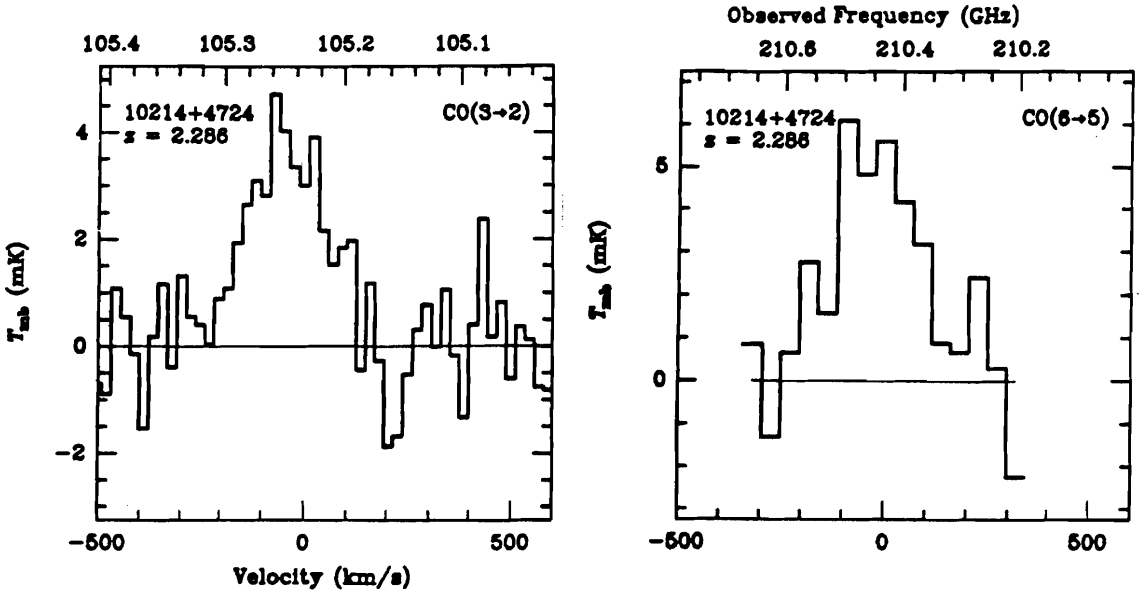

Figure 1. The ^{12}CO (3–2) and (6–5) line profiles of IRAS10214+4724, observed with the IRAM 30 m telescope (from Solomon et al. 1992). The lines, the rest frequencies of which are 346 GHz and 692 GHz, are redshifted to 105 GHz and 210 GHz, respectively

How much faith can we put in this gas mass estimate and what is exactly the 'standard Galactic' $N(H_2)/W(CO)$ conversion factor will be the main subject of this lecture.

You may ask why not simply use the 21 cm line to study such high redshift objects. There are two reasons for this: firstly, the 21 cm line traces the atomic, not the molecular gas, and, we believe, the latter is more abundant; secondly, the 21 cm line is redshifted to 430 GHz, a frequency where the sky is noisy and the radio telescopes have a poor sensitivity. It is worth noting that even forgetting about abundances and redshift, the 21 cm line is more difficult to detect than the CO millimeter lines in an object of small angular dimensions. Indeed, the 21 cm line excitation temperature is only a factor of $\simeq$ 2–5 larger than that of the CO lines; the 21 cm line opacity, on the other hand, is much smaller. As I_ν, the line intensity scales as $T_{ex}\nu^2(1-e^{-\tau_\nu})$ (see below), the 21 cm line will be $> 10^3$ times weaker than the 2.6 mm line of CO. Even allowing for differences in atmosphere transparency and detection techniques, it requires a telescope with a $\sim$ 10 times larger diameter

to detect the line emission of an unresolved source (or to study an extended source with the same angular resolution). The IRAM interferometer, shown on Fig. 2, which operates at mm wavelengths, should be replaced by three 150 m diameter dishes to be able to study the 21 cm line with an equivalent sensitivity and the same angular resolution. No doubt, millimetre wave observations will play a large role in future studies of remote extragalactic objects.

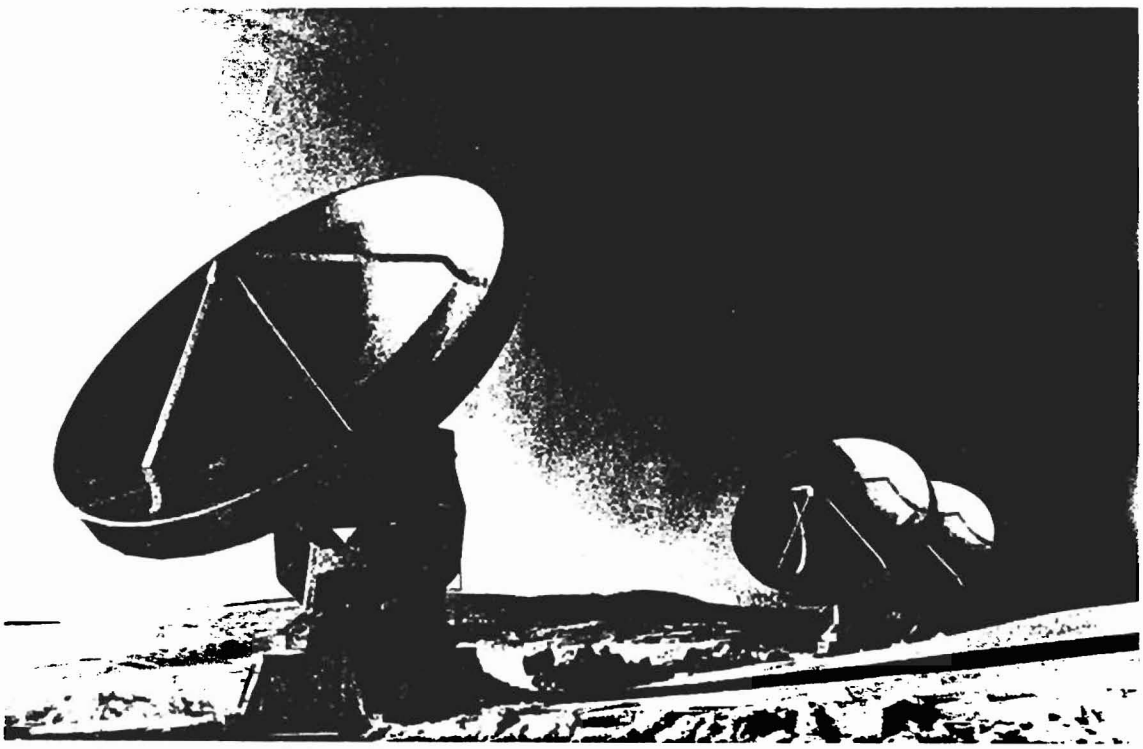

Figure 2. The IRAM millimeter interferometer on Plateau de Bure in 1991 (from Guilloteau et al. 1992). Since Feb. 1993, this instrument includes a 4th 15-m diameter antenna.

Spectroscopy and Radiative Processes

Atomic hydrogen

The hydogen atom has a simple energy level diagram described, in the first approximation, by Sommefield's equation.

Its lowest electronic state, the $n = 1$ state, is called $1S$. For $n > 1$, several levels (fine structure levels) with slightly different energies exist (e.g. $n = 2, l = 0(2S), l = 1(2P)$– see Herzberg 1945, p. 26). These, however, lie all > 82000 cm^{-1} (or $> 10^5$ K) above the ground ($n = 1, l = 0$) electronic state. Their population is negligible in the general interstellar gas and almost all H atoms are in the $1S$ state. *

Although a single spherical electronic orbital is allowed in the $n = 1$ state, the electron spin can take two different orientations with respect to the nuclear spin: parallel or antiparallel. The energy of the system, in the first case, is very slightly higher (by 0.047 cm^{-1}, or [21 cm]$^{-1}$) than in the latter case. The difference in energy is very small because it involves weak coupling forces between the magnetic moments associated with the electron and the nucleus, which should be considered as rotating charged spheres of very small, but finite radii. The $1S$ state has thus of two 'hyperfine' sublevels with statistical weights 3 and 1. Collisional transitions between these two levels are easy, since the levels are very close and since the spin momentum can be preserved at the expense of the colliding particle; pure radiative transitions, on the other hand, lead to a change of spin and are strictly forbidden. The populations of the two sublevels distant by 0.07 K are therefore thermalized in about every conditions (i.e. they are in the same ratio as their statistical weights).

Strictly forbidden does not mean impossible. The Einstein A_{10} coefficient is only extremely small: $A_{10} = 2.85\ 10^{-15}$s^{-1}. The lifetime of the upper level against spontaneous de-excitation is 10^7 year (vs 0.5 y for the $J = 1 - 0$ rotational line of CO). Since atomic hydrogen is very abundant in the interstellar medium (ISM)

* Throughout this lecture, we will discuss a wide range of energies. It is customary, in optical/IR spectroscopy to express the energies E of the levels in cm^{-1} (in which case, we speak of wavenumbers $E/hc = \lambda^{-1}$, rather than of energies) and in microwave spectroscopy in kelvin (in which case we speak of temperatures E/k). Line 'frequencies' are expressed in cm^{-1} in the FIR and in MHz or GHz in the radio domain. Correspondances between these units are: 1.46K $\Leftrightarrow$1 cm^{-1} $\Leftrightarrow$ 30 GHz.

and since about all H atoms are in one of the two $1S$ sublevels, the 21-cm line ISM emission is fairly strong and easily observed.

Because A_{10} is so small, the 21 cm line is often optically thin. The integrated line intensity is then expressed by:

$$\int I_\nu d\nu = \int\int j_\nu d\nu dl = \int \frac{1}{4\pi} n_1 A_{10} h\nu dl.$$

Since the populations of the higher states are very low and the $1S$ ground state almost always thermalized the population of the $1S$ upper level, n_1 is just 3/4 n_{tot}. The column density of HI along the line of sight, $N(HI)$, is then simply proportional to the integrated line intensity:

$$N(HI) = \int n_{tot} dl = 1.82\ 10^{13} \int T_B dv,$$

(where $N(HI)$ is in at.cm^{-2} and $\int T_B dv$ in K.kms^{-1}). As standard in radio astronomy, the line intensity I_ν has been replaced by the Raleigh-Jeans 'brightness temperature' $T_B = (\frac{2\nu^2 k}{c^2})^{-1} I_\nu$ and $d\nu$ by $\frac{\nu}{c} dv$.

When the line is optically thick, the above expression becomes:

$$N(HI) = \int n_{tot} dl = 1.82\ 10^{13} \int T_B \frac{\tau}{(1-e^{-\tau})} dv \quad \text{with} \quad \tau \approx -ln(1 - \frac{T_B}{T_{ex}}).$$

Spectroscopy of H_2 and CO

Fig. 3b (from Herzberg 1950) shows the energy diagram of the lowest electronic states of the H_2 molecule. The ground state is the state in which both electrons are in the lowest orbital, $1s\sigma$. It is denoted $^1\Sigma^+$, by analogy with the 1S state of atomic H. The excited states, like in the case of HI, have large energies and are not populated in the general ISM. Absorption lines from the ground $^1\Sigma^+$ state to higher $^1\Sigma$ states (the Lyman lines) can be observed in the line of sight to bright stars, but only from space-borne telescopes, since these lines lie between 1215 A and 912 A, in

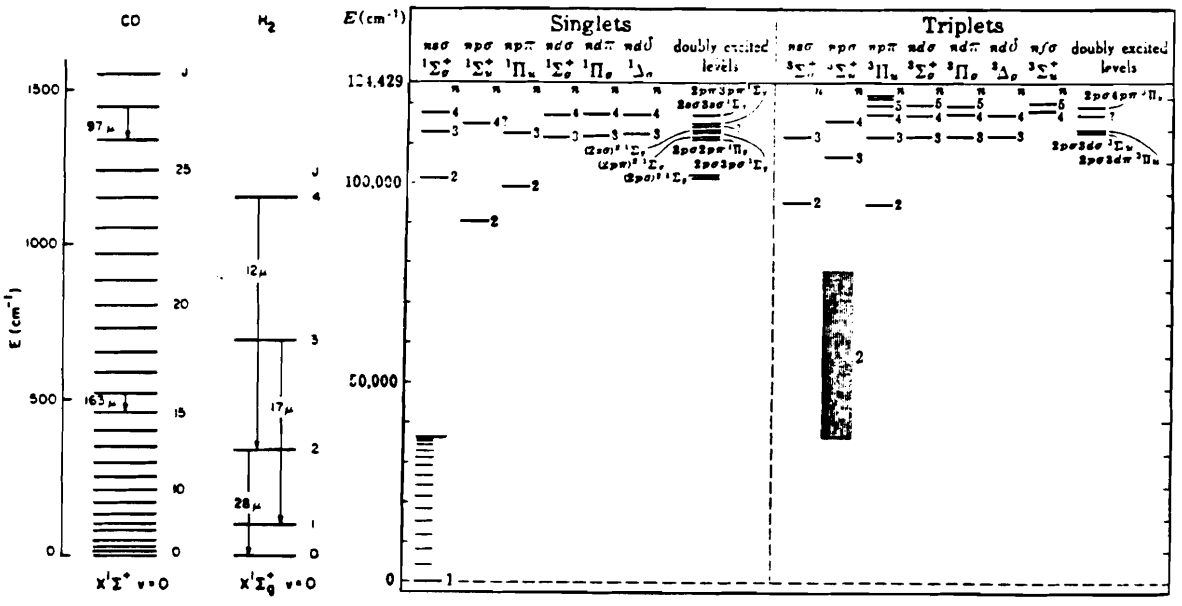

Figure 3. **a.** Rotational levels of the ground electronic and vibrational states of CO and H_2 (from van Dishoeck and Black 1987). **b.** Energy diagram of the electronic states of H_2 (from Herzgerg 1950, p.340)

the far UV. To date, the ISM absorption has been measured toward a few hundred stars, mostly with the Copernicus and IUE satellites (see e.g. Fig. 4).

The ground electronic state of H_2 consists of different vibrational states split into a series of rotational levels. Because of the de-coupling of electronic and nuclear motions, these latter, at least the lowest ones, are well described by the eigenlevels of a vibrating rotator: $E_v = \omega_e(v + 1/2)$ for the vibrational states, $E_r = B_v J(J+1) + DJ^2(J+1)^2$ for the rotational states, where v and J are the vibrational and rotational quantum numbers and where ω_e is the vibration frequency and $B = h/8\pi^2 I$ the rotation constant (I is the molecular moment of inertia –e.g. Herzberg 1950). The vibrational states $v > 0$ have energies of thousands of K and are not populated under normal ISM conditions.

The rotational levels of the H_2 ground state are shown in Fig. 3a. H_2 has two identical nuclei and no permanent dipole moment. Radiative and collisional

transitions between odd and even J levels are strictly forbidden. H_2 can be seen as two different species, one with even J levels, para H_2 ($J = 0, 2, 4...$), and one with odd J levels, ortho H_2. Transitions within each species are allowed –in particular, the electric quadrupole transitions within the v=0 state, which obey the rule $\Delta J=2$ (see Fig. 3a and Herzberg 1950, p. 131).

The lowest H_2 transition is the $J = 2 - 0, v = 0$ transition. Its frequency is $6B = 179$ cm^{-1}, its wavelength 28 μm. The $J = 2$ level lies 500 K above the ground level and is scarcely populated in molecular clouds. Except for shocked gas regions, the H_2 infrared lines, as the H_2 UV lines, are thus observed only in absorption in the lines of sight to a few bright sources and are poor probes of the general ISM.

The latter is better studied with other molecules and more particularly CO.

CO is much heavier than H_2 and has a smaller B: its rotational levels are thus more tightly packed (Fig. 3a). It has also a non-zero permanent electric dipole moment ($\mu = 0.12$), so that $\Delta J = 1$ transitions within its ground state are allowed. The lowest transition ($J = 1 - 0$) has a frequency of 115.3 GHz (3.8 cm^{-1}, or 2.6 mm); the next ($J = 2 - 1$ and 3-2), frequencies of 230.5 GHz (1.3 mm) and 345.8 GHz (0.87 mm); all lie in fairly transparent atmospheric windows and can be observed rather easily from the ground. The $J = 1, 2$, and 3 levels have energies of 5.6 K, 17 K and 33 K. They sample nicely the range of temperatures encountered in molecular clouds. The 1–0 line is observed in emission in about every molecular cloud; the 3–2 line is strong only in the dense (>3000 cm^{-3}) and warm (T> 30 K) clouds (unless the 1–0 and 2–1 line opacities are very large).

The opacity τ_ν of the CO $u \rightarrow l$ line is given by (e.g. Spitzer 1978, p.36):

$$\int \tau_\nu d\nu = \int \kappa_\nu dl d\nu = \int \frac{h\nu}{c}(n_l B_{lu} - n_u B_{ul})dl = \int \frac{h\nu}{c} n_l B_{lu}(1 - e^{\frac{-h\nu}{kT_r}})dl,$$

where T_r, the 'rotation' temperature, describes the population of the lowest (i.e. most populated levels). Note that, for CO, $T_r \simeq T_k$ as soon as the local gas density n(H_2) > 3 10^3 cm^{-3}.

Since,

$n_l \simeq n_{tot}\frac{hB}{kT}(2J+1)e^{-\frac{E_l}{kT_r}}$ and $B_{lu} = \frac{8\pi^3(J+1)}{3h^2(2J+1)}\mu^2$,

$$\tau_\nu = \tau_o \Phi(\nu) = \frac{\Phi(\nu)}{\Delta\nu}\int \tau_\nu d\nu = \frac{\Phi(\nu)}{\Delta\nu}\int \frac{4\pi^3\mu^2\nu^2}{3kTc} e^{-\frac{E_l}{kT_r}}(1 - e^{\frac{h\nu}{kT}})dl.$$

For an homogeneous cloud,

$$T'_B(\nu) = T'_{bg}e^{-\tau_\nu} + T'_r(1 - e^{-\tau_\nu}),$$

and for an optically thin cloud,

$$W(\mathrm{CO}) = \int T'_B dv = 1.44 \cdot 10^{-16} N(CO) \frac{T'_r - T'_{bg}}{T_r T'_r} \mu^2 \nu^2 e^{\frac{-E_u}{kT}},$$

where the 'prime' denote Raleigh-Jeans temperatures, $T' = \frac{h\nu}{k}(e^{\frac{h\nu}{kT}} - 1)^{-1}$, and where $T_bg = 2.7$ K is the Cosmic background temperature. Note that $T'_{bg} = 2.2$ K.

In the case $T_r >> \frac{h\nu}{k} > T_{bg}$ (or >>6 K, in the case of the 1-0 line of CO), the above equation becomes:

$W(\mathrm{CO}) = \int T'_B dv = 1.44 \cdot 10^{-16} N(CO) {T_r}^{-1} \mu^2 \nu^2 e^{\frac{-E_u}{kT}}$

(T is in kelvin, dv in kms^{-1}, $\mu = 0.112$ D in debye, and ν in GHz. N(CO) is in cm^{-2}).

The derivation of N(CO), contary to that of N(HI), requires the knowledge of T_r even in the optically thin case. Moreover, the millimetre lines of the the most abundant CO isotope, ^{12}CO, are seldom optically thin: for an homogeneous cloud with T_r= 20 K and Δv= 1 kms^{-1}, $\tau > 1$ as soon as $N(CO) > \int n_{tot} dl = 2\ 10^{16}$ cm^{-2}.

In the case of optically thick lines, the population of the rotational levels, hence T_r, depend on τ. In order to find $T_B(v)$, one has to resolve simultaneously the statistical equilibrium equations and the radiative transfer equations across the cloud. If the physical parameters and the molecular abundances are known throughout the cloud, this resolution can be done iteratively e.g. by using Monte Carlo techniques (Bernes 1978). When these parameters are poorly known, one ususally assumes constant the gas density, kinetic temperature and fractional CO abundance, x(CO), and assumes radiative decoupling between the different parts of the cloud (the so-called Large Velocity Gradient, or LVG approximation). Locally, the line opacity is taken care of in the statistical equilibrium formula by dividing by $\sim \tau(i)$ the escape probability of a photon from the cell (i) where it is emitted; $\tau(i)$ is the opacity in the cell: the photons leaving the cell, because of the velocity gradient, escape freely from the cloud (Goldreich and Kwan 1974).

Extinction and emission of Dust Grains

The presence of interstellar dust is revealed by the observation of dark areas with sharp boundaries in the Milky Way. These 'dark nebulae' are nothing but

nearby interstellar clouds, composed of gas and of tiny dust grains, which absorb the light from background stars. Star counts, i.e. the study of the number of stars, per unit area, as a function of their apparent intensity (or 'magnitude', in the logarithmic scale) in the obscured regions and in a reference field, yield the dust average optical depth, τ_λ (or 'extinction' A_λ, in the logarithmic scale), at the wavelength(s) at which the observations were made. Star counts are usually made on optical plates in the V band (i.e. taken with filters centred at 5550 Å), and the derived opacity (extinction) is referred to as 'visual'. The relation between the visual optical depth, τ_v and the 'visual extinction', A_v stems from the astronomical definition of the 'magnitude' and is simply $A_v = 1.086\tau_v$ (see Spitzer 1978, chap. 7 for a comprehensive description of absorption by IS dust). Obviously,

$$\tau_v = \int n_g \sigma_g Q_e dl = < n_g \sigma_g > Q_e L \quad (1),$$

where n_g and σ_g are the dust grain volume density and geometric cross section. $Q_e(\lambda)$, the extinction effiency factor (see Spitzer 1978), is simply 2 for dust grains of size $a >> \lambda$ (Babinet's principle). L, finally, is the size of the cloud.

When $a \leq \lambda$, $Q_e(\lambda) \sim \lambda^{-1}$; τ_v and A_v scale as λ^{-1} and the stars located behind a dust cloud appear redder. This 'reddening' $A_{\lambda 1} - A_{\lambda 2}$ (E_{B-V} when the two wavelengths are respectively 4350 Åand 5550 Å, the centres of the 'blue' and 'visual' bands) can be accurately measured for bright stars of known spectral type; from it, one can derive A_v and τ_v.(Ususally, one finds $A_v \simeq 3\ E_{B-V}$.)

Star counts and reddening measurements against one thousand of stars of known distance and spectral type yield $A_v/L \simeq 3E_{B-V} = 0.6$ mag kpc^{-1}, form which one derives (through eq. (1)) $< n_g \sigma_g >= 3\ 10^{-22}$ cm^{-1}.

Note that the knowledge of $< n_g \sigma_g >$ allows to calculate the timescale, of great interest for chemical studies, for a given H atom to hit a dust grain:

$t_g = (w_H < n_g \sigma_g >)^{-1} \sim 2\ 10^{16}/n$ s, where
$w_H = (8kT/\pi m_H)^{1/2} = 1.46$ kms^{-1} for $T = 100$ K, is the velocity of the H atom relative to the (much more massive) dust grain.

A very important empirical relation is that between the gas column density, N(HI+2H_2), and the reddening, E_{B-V}, in 'diffuse' clouds (i.e. clouds for which $E_{B-V} < 0.6$, or $A_v < 2$). This relation was first established for the mostly atomic clouds, but is found to apply also to the diffuse molecular clouds. Fig. 4, from Bohlin et al. (1978) shows the correlation established for 100 stars, mostly located within 2 kpc from the sun, between E_{B-V} and either N(HI) (*left figure*) , or N(HI+2H_2) (*right*). The two latter quantities were derived from the Lyman α line profiles of

atomic and molecular hydrogen, observed with the Copernicus satellite. The data points in the right graph lie almost all within a factor 1.5 of the straight line:

$$N(HI + 2H_2)/E_{B-V} = 5.8\ 10^{21} \text{at.cm}^{-2}\text{mag}^{-1},$$

which corresponds roughly to $N(HI + 2H_2)/A_v = 1.8\ 10^{21} \text{at.cm}^{-2}\text{mag}^{-1}$.

There are arguments (see e.g. Cernicharo & Guelin 1987) showing that the above relation also extends to 'translucent' clouds (i.e. clouds with $A_v = 1 - 4$).

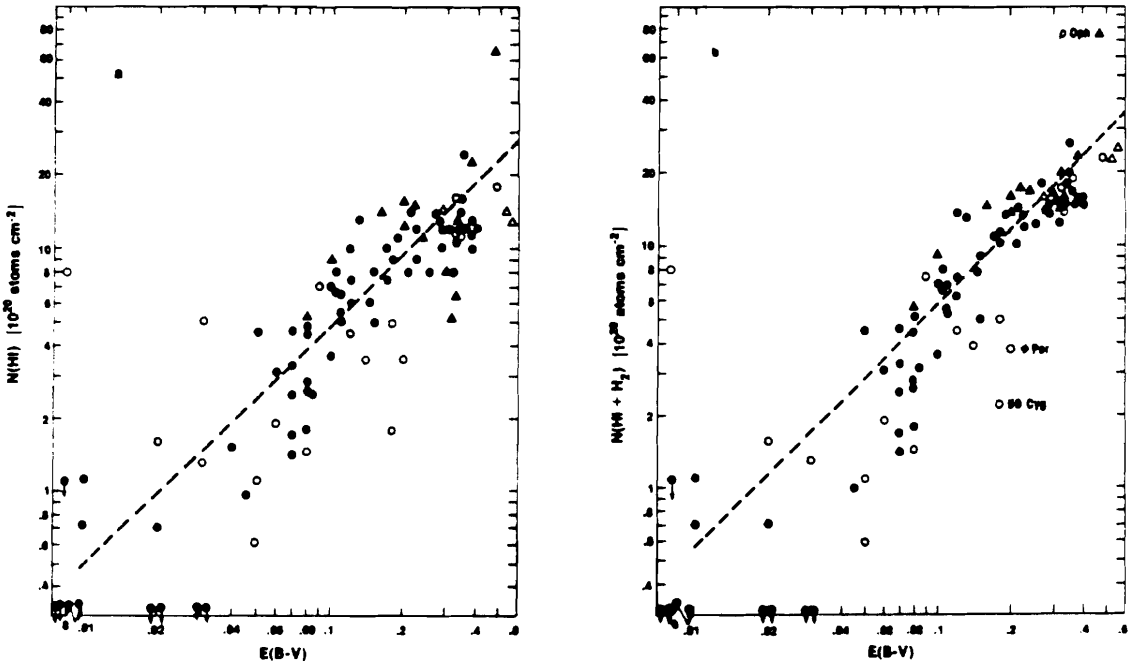

Figure 4. The correlations between E_{B-V} and N(HI) *(left)* and N(HI+2H$_2$) *(right)* derived by Bohlin et al. (1978)

The mass of IS dust, in the vicinity of the Sun, is estimated to be between 1 and 2% of the mass of the gas.

Dust grains, of course, not only absorb and scatter the light, but also re-emit the absorbed radiation. This emission occurs mostly in the IR for hot dust (> 1000 K) and in the FIR or submillimeter ranges for warm (30–100 K) and cold (10–20 K) dust. This emission can be used to estimate the dust opacity, hence its column

density and the gas column density (e.g. using Bohlin et al.'s relation). This has been done by several authors (see e.g. Cox and Mezger 1983, Hildebrand 1983).

For example, Mezger et al. (1990) arrive, for the Galactic molecular clouds, at the relation:

$$N(H_2) = 1/2N(H) = 10^{22} S_{1300} \frac{e^x - 1}{T_d x},$$

where S_{1300} is the 1.3 mm flux density in a 12"-wide beam, expressed in millijansky, T_d the dust temperature, and x=11.1/T_d.

Note that the column densities derived by this method depend critically on the dust properties, and in particular on its temperature: IR measurements are blind to cold dust and the millimeter measurements relatively insensitive to hot and warm dust. In practice, the dust temperature may vary considerably across a given cloud.

Interstellar Chemistry

Formation of the H_2 Molecule

Hydrogen is by far the most abundant element, especially as concerns elements composing molecules. Most of the molecular gas is thus in the form of H_2.

Obviously, the simplest way to form an H_2 molecule is by association of 2 colliding H atoms. In the gas phase, the timescale for a given H atom to collide with another atom is $t_{col} \sim 10^{10}/n$ s, where n is the gas density expressed in cm^{-3} (Watson 1975). This time, in a HI cloud ($n = 10 - 100$ cm^{-3}) is typically 10^3 y, much shorter than the age of the cloud. Simple 2-atom collisions, however, do not form a stable H_2 molecule, since the formation energy (4.5 eV in the ground state –see Fig. 5) must first be expelled.

Emission of a photon (i.e. direct radiative association) is not possible, since the only repulsive state with energy close to 0, the $^3\Sigma$ state, is not radiatively connected to the ground $^1\Sigma$ state (this would require a change of electronic spin!).

In laboratory experiments, the excess energy is evacuated by a 3 rd particle or by the walls of the apparatus. In IS space, the density is too low for 3-body collisions ($t_{3by} \geq 10^{31}/n^2$ s, i.e. more than the age of the Galaxy for a typical cloud) and there are no walls. Dust grains, however, do play the role of the latters.

We have seen that the timescale for a given H atom to hit a dust grain is $t_g \sim 2\ 10^{16}/n$ s. For $n = 10^5$ cm^{-3}, a few H atoms will hit a dust grain per cm^{-3}

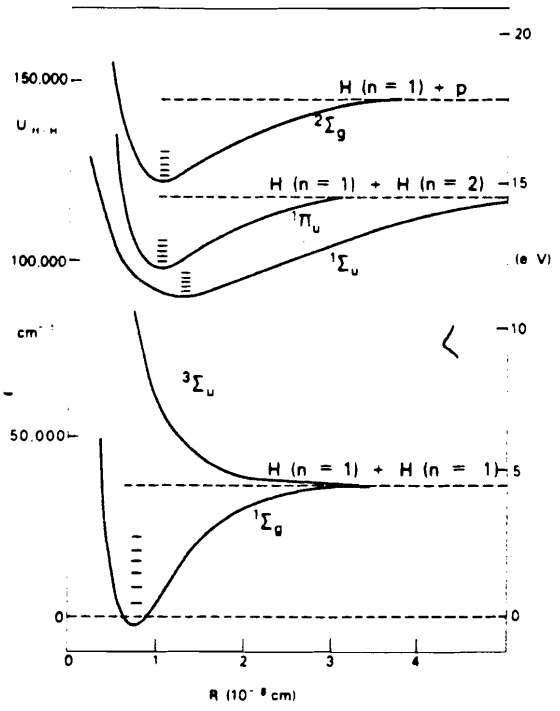

Figure 5. Potential energy curves for low lying states of H_2 (from Watson 1975, p.235)

per year, enough to convert all the H atoms into molecules in a few thousand years, provide every second collision leads to the formation of an H_2 molecule.

For this to happen, other conditions must be fullfilled (Watson, ibid), the most important being the dust grains are cold enough for the evaporation time be larger than the time t_g needed for a second H atom to stick. In practice, this means $T_g < 20K$.

An alternate formation process exists in the pure gas phase ($H+H^- \rightarrow H_2+e$), but this process is typically a factor of 10^3 less efficient.

The ionization potential of H_2, 15.4 eV, is larger than that of HI; the destruction of H_2, at least in diffuse clouds results mostly from photodissociation.

Due to the H_2 structure (Fig. 6), photodissociation in the ISM UV field occurs only through a 2-step process involving i) an upwards transition from the ground $^1\Sigma^+$ state to a higher bound electronic state, followed by ii) a radiative de-excitation to vibrationally excited states leading to the molecule dissociation.

Because this process involves absorption in narrow lines relating two bound states, it becomes inefficient as soon as one deepens into a cloud and the UV radiation gets absorbed at the line wavelengths: H_2 is said to self-shield against photodisssociation. The H_2 abundance relative to HI increases then rapidly.

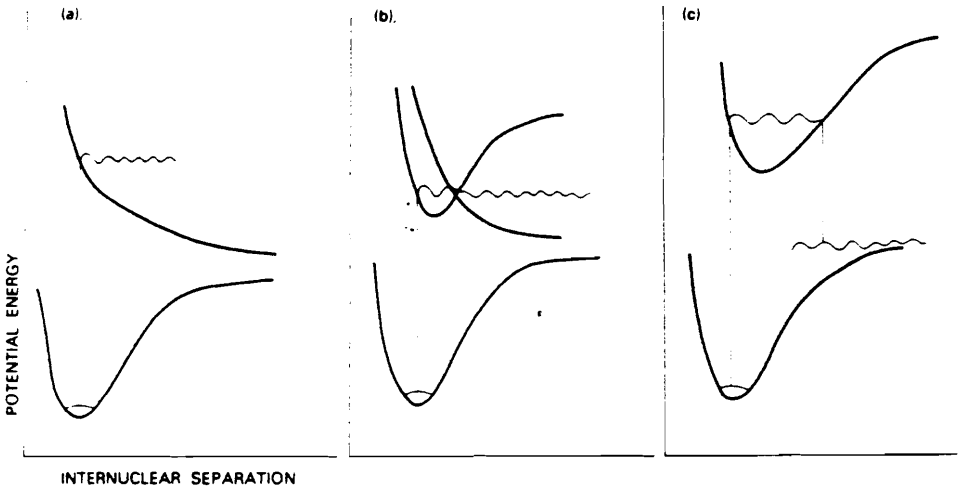

Figure 6. Molecular potential energy curves illustrating the 3 modes of photodissociation. Only case (c) applies for the $^1\Sigma^+$ ground state of H_2 (from Watson 1975)

H_2 is a simple enough system for this process be calculated with some accuracy. In the unshielded 'standard' IS radiation field, the H_2 molecule lifetime is $\simeq 10^3$ y (rate k_{pd}= 5 10^{-11} s^{-1}). It raises to 10^6 y inside a layer of 3 10^{20} H_2 molecules cm^{-2} (or A_v= 0.3 mag). Fig. 7, from van Dishoeck and Black (1988) shows the decrease of k_{pd} as one deepens into a cold cloud with n= 1000 cm^{-3}. A sharp drop of k_{pd} is predicted at depths 1-3 10^{20} cm^{-2} ($A_v = 0.1-0.3$), accompanied by a parallel drop of the HI abundance and a steep increase of the H_2 abundance. For $A_v >> 0.3$, almost all hydrogen is in the form of H_2.

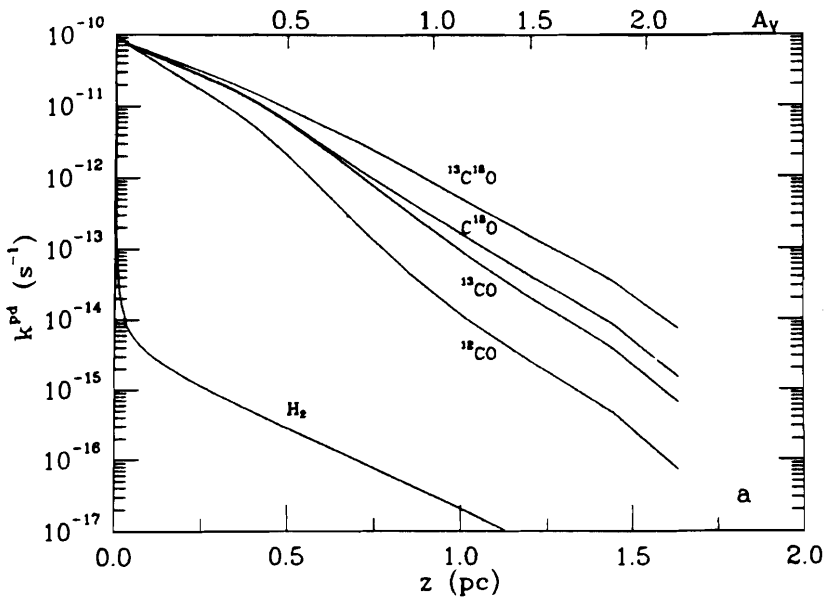

Figure 7. Photodissociation rates of H_2 and the different CO isotopomers as functions of linear depth into a translucent cloud (from van Dishoeck and Black 1988)

Observations of the Lyman H_2 and HI lines in the line of sight to the bright nearby stars confirm the steep increase of the H_2 abundance at $A_v = 0.3$ mag.

Formation of the CO Molecule

In diffuse clouds, the formation of CO is thought mostly to result from the fast reaction $OH + C^+ \rightarrow CO + H^+$. CO is chemically very stable and its ionization potential is large (14 eV). Like H_2, it is essentially destroyed by photodissociation.

The dissociation energy of CO is 11.1 eV, so that photons with $\lambda < 1120$ Åare required for its photodissociation. As the IS radiation is absorbed below 912 Å, the wavelength range of interest is 912-1120 Å.

This portion of CO spectrum has been explored with a spectral resolution high enough to resolve the absorption lines from the continuum absorption (Letzelter et al. 1987, 1988). The absorption spectrum shows only lines, which implies that direct transitions to repulsive states do not occur at these wavelengths. In fact, the CO dissociation mostly results from transitions to predissociated bound states (van Dishoeck and Black 1988). CO, like H_2, can self-shield against photodissociation, but less efficiently that the latter molecule: the CO predissociation times are 10^3 times shorter than the radiative times and its upper states are broad. The absorption lines responsible of the CO photodissociation are broader than in the case of H_2,

hence more difficult to saturate; the effect is strengthened by the low abundance of C and O, relative to H.

Calculations (van Dishoeck & Black 1988– see Fig. 7) based on experimental dissociation cross sections show that the photodissociation rate of CO decreases more slowly than that of H_2 when one moves into a cloud. It is only at depths > 10^{21} H_2 molecules, i.e. for $A_v \geq 1$ mag. that CO self-shields efficiently and that its abundance raises to reach (in steady state) 1-2 10^{-4} of that of H_2; about all the carbon available in the gas is then locked into CO molecules. For $x(CO) = 10^{-4}$, T_k= 20 K and Δv= 1 kms^{-1}, the 1–0 line of ^{12}CO becomes optically thick as soon as one deepens an extra $\Delta N(H_2) = 2\ 10^{20}$ cm^{-2}, or ΔA_v =0.2 mag., which is very little.

The upwards transitions to predissociated states involve vibrationally excited states. The absorption spectra of the different CO isotopomers, ^{12}CO, ^{13}CO, and $C^{18}O$, which have different vibration frequencies, are not coincident. Mutual shielding (e.g. of ^{13}CO by the more abundant ^{12}CO isotopomer) is thus only partial. ^{13}CO and $C^{18}O$ being 50–500 less abundants than ^{12}CO, self-shielding occurs much deeper into the cloud or not at all. Despite some partial shielding by ^{12}CO and even H_2, ^{13}CO and $C^{18}O$ become abundant only where the UV radiation has almost vanished (van Dishoeck and Black 1990).

Observations of the ^{12}CO, ^{13}CO, and $C^{18}O$ line intensities at the edge of molecular clouds are in qualitative agreement with the above. The three isotopomers become detectable at different depths or 'thresholds' (Fig. 8). Quantitatively, however, the observed thresholds agree poorly with the calculated ones, especially when line excitation is taken into account (Guelin and Cernicharo 1987, van Dishoeck and Black 1990).

The Empirical W(CO) to N(H_2) conversion factor in the Milky Way

From the above, it is clear that i)the millimeter lines of ^{12}CO are optically thick in almost all 'dense' molecular clouds, ii)that in such clouds their intensity depends on the gas temperature more than on the CO column density, and iii) that the CO column density does not necessarily reflect the H_2 column density (since CO may still be photodissociated at the periphery of molecular clouds). Normally, one shouldn't then expect any simple relation between $W(CO)=\int T_b'(CO)dv$ and N(CO), and *a fortiori* between W(CO) and N(H_2).

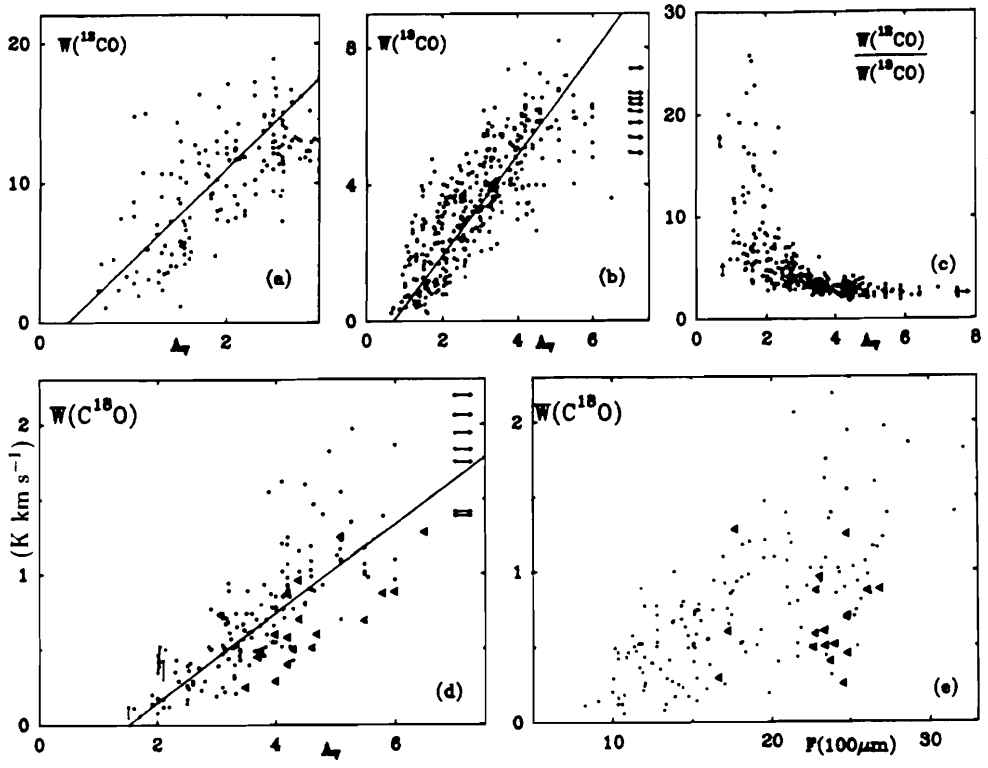

Figure 8. a to d: the CO integrated temperature–visual extinction correlation diagrams in Heiles' Cloud 2. Note the different thresholds for the detection of ^{12}CO, ^{13}CO and $C^{18}O$ (from Guelin and Cernicharo 1987)

Yet, curiously, several observational results point toward such a relation, as first noted by Liszt (1982).

The Virial Mass- CO luminosity relation

In an analysis of their $^{12}CO(1–0)$ survey of the galactic plane, made with the FCRAO 14.7 m antenna, P. Solomon and collaborators (e.g. Solomon and Rivolo, 1987) report having resolved some 300 molecular clouds (or bound cloud complexes). Comparing the masses of these clouds derived from the sizes and linewidths (the 'virial masses' M_{vt}) to the cloud 'CO luminosities' (or CO intensity integrated over

velocity and over the cloud area, $L(CO) = \int T'(CO) dv dx dy$ in K kms^{-1}pc^2), they find an (astonishingly!) good correlation (see Fig. 9). It yields

$M_{vt} = 39(L(\mathrm{CO}))^{0.81} M_\odot$,

or, on the average, $\mathrm{N(H_2)} = 3\ 10^{20} W(\mathrm{CO})$, where the 'conversion' factor (hereafter denoted X) is expressed in $\mathrm{H_2}$ mol cm^{-2} K^{-1}km^{-1}s.

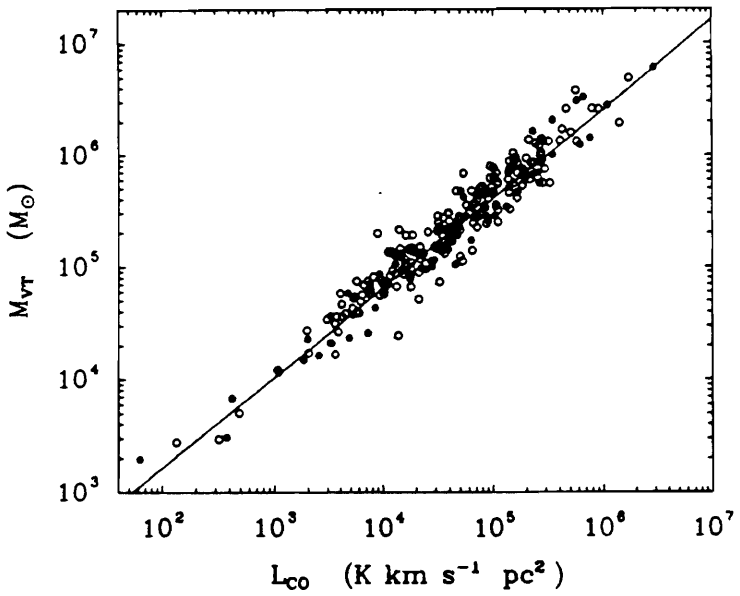

Figure 9. The virial mass–CO luminosity relation for Galactic molecular clouds, according to Solomon and Rivolo (1987)

The 'virial mass' is the mass of a spherical cluster of compact clouds, at equilibrium under its own gravity. Ignoring any other force, the Virial Theorem can be expressed by $M_{vt} = kR\Delta v^2$, where $\Delta v = \sqrt{2} \times r.m.s.cloudvel.$ is the FWHP velocity along the line of sight, expressed in kms^{-1}, R is the cloud radius in parsec, and k a numerical factor $\simeq 200$ which depends on the radial mass distribution $\rho(r)$ in the cluster (e.g. $k = 190$ for $\rho(r) \sim 1/r$, MacLaren et al. 1988).

Gamma-ray gas mass determinations

The diffuse gamma ray radiation, mapped e.g. by the COSB satellite, mostly results from the interaction of cosmic rays with the hydrogen nuclei in the IS medium.

If the cosmic ray distribution is constant along the line of sight, its intensity can be expressed by

$$I_\gamma = q_\gamma(2\mathrm{N(H_2)}+\mathrm{N(HI)}),$$

where q_γ is a parameter to be determined. The Gamma ray studies yield I_γ for a few individual, nearby clouds, as well as for the background of remote Galactic clouds. In the direction of diffuse, mostly atomic clouds, (2N(H_2)+N(HI)) reduces to N(HI), which can be measured by mapping the 21 cm line emission. The value of q_γ can then be derived. Assuming the cosmic ray distribution is known (e.g. constant), the above equation can be used in turn to derive N(H_2) in the regions where the gas is mostly molecular. The values of N(H_2) derived by this way can then be compared with the velocity-integrated CO intensities, W(CO).

Such a comparison was made by two teams (the COSB team and the University of Durham team) with somewhat diverging results. Strong et al. (1988) find that $\mathrm{N(H_2)} = (2.3 \pm 0.3)\ 10^{20}\mathrm{W(CO)}$ (in the same units as above) reproduces well the γ–ray and CO data (namely the COSB survey and the Columbia ^{12}CO $J = 1-0$ galactic plane survey) as well for the gas in the solar neighborhood, as for the gas in the inner parts of the Galaxy. Bhat et al. (1986–see also MacLaren et al. 1988), on the other hand, find values of X= N(H_2)/W(CO) 1.5–2.5 times smaller and a clear decrease of X from the solar neighborhood to the Inner Galaxy.

It should be noted that the γ–ray method tends to oversetimate X, since the diffuse γ–ray emission may be blended with the emission of background point sources (pulsars,...) and since the cosmic ray density could be enhanced within the clouds (see Strong et al. 1988).

Gas masses derived from star counts and ^{13}CO observations

The mass of the nearest molecular clouds can also be derived using star counts for the less opaque clouds, and ^{13}CO for the darkest clouds. This method was in applied, in particular, to the nearby (D = 100 – 200 pc) Taurus complex of dark clouds (Guélin and Cernicharo 1988). The mass of gas in the diffuse/translucent region of this complex was calculated from the average visual extinction derived from star counts (A_v = 1.8 mag.), using Bohlin et al's N(H)/A_v relation. The mass of the opaque region (A_v > 4 mag) derived from an alaysis of the excitation of the optically thin ^{13}CO and C^{18}O millimeter lines, is relatively small ($\leq$ 1/5 of the total). Comparing the masses (5800 M_o in total) with its ^{12}CO(1–0) 'luminosity',

measured by Ungerechts and Thaddeus (1987) with the Columbia telescope, Guélin and Cernicharo find

$X = 2.2\ 10^{20}$ H_2 mol cm^{-2} K^{-1}km^{-1}s.

in surprisingly good agreement with the γ-ray value derived by Strong et al. (1988).

Note that a derivation of the mass of the entire complex solely based on ^{13}CO would have yielded a mass and a X factor twice smaller, adopting the 'canonical' fractional abundance $x(^{13}CO) = 10^{-6}\ x(H_2)$.

In summary, independant estimates of the $X = N(H_2)/W(^{12}CO\ 1\text{–}0)$ ratio for nearby and for remote molecular cloud complexes point toward a value of this ratio which would be constant within a factor of 2 across the Galaxy. The average ratio $X = 2.3\ 10^{20}$ H_2 mol cm^{-2} K^{-1}km^{-1}s is often called the 'standard Galactic CO to H_2 conversion factor'.

Possible justifications and criticisms

Several interpretations have been advanced to explain (and mostly comfort) the existence of this empirical proportionality factor. The first assumes that the clouds are statistically identical and small enough not to shadow one another along the line of sight. In this case, the CO luminosity merely counts the number of clouds intercepted by the beam, and is proportional to the molecular mass. A more sophisticated explanation has been advanced by Dickman et al. (1986 – see also van Dishoeck and Black 1987). It assumes that the clouds (mostly dense GMCs) are in virial equilibrium and that CO is thermalized . Neglecting cloud-cloud shadowing, W(CO) is proportional to $N(H_2)T_{ex}/\sqrt{\rho}$, where ρ is the volume density and T_{ex} the excitation temperature. Note that the dependance of X on $T_{ex}/\sqrt{\rho}$ is 'robust' in the sense that the excitation temperature tends to to be larger in the densest parts of the giant molecular clouds (e.g. the OMC1 'core' in Orion).

A third explanation proposes that the molecular gas is dominated by relatively low density halos, where CO is subthermally excited (Guélin and Cernicharo 1987). Monte Carlo radiative transfer calculations, for "realistic" halo (+small core) models inspired by the clouds in the Taurus region, show the CO intensity to increase almost linearly with $N(H_2)$ along most lines of sight (see e.g. Fig. 10); the derived proportionality factor is close to the observed one (Guélin and Cernicharo 1988). Basically, the bulk of the gas lies in regions with $n(H_2)$=100–300 cm^{-2}, half-way between the "low excitation" regime (where $A/\tau >> C$ and the optically thick line

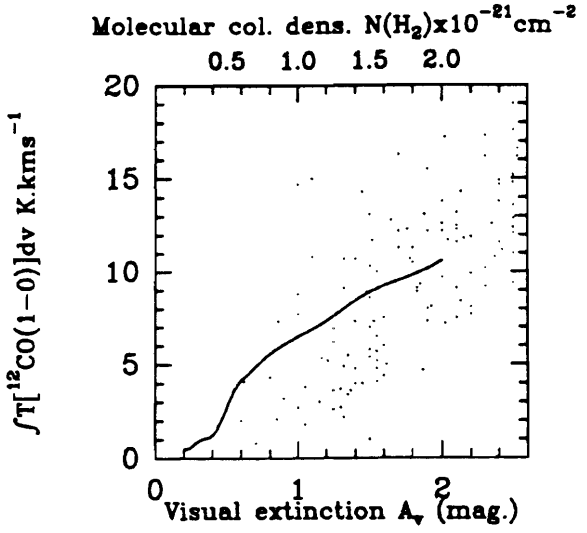

Figure 10. The ^{12}CO integrated intensity across a cloud, plotted as a function of the H_2 column density along the line of sight. The data points are extracted from the ^{12}CO observations shown in Fig. 8. The line is a Monte Carlo calculation for a model spherical cloud (from Guelin and Cernicharo 1988)

intensities still proportional to the molecular column density), and thermalization, where T_{ex}=Cst.

More and more, observations tend to show that, at large scales, the molecular mass lies mostly in cloud halos (presumably far from virial equilibrium), hence to support the last model (see e.g. Garcia-Burillo & Guelin 1993): the ^{12}CO and ^{13}CO J=(2–1) and (1–0) line intensities observed in the Taurus region as well as in nearby galaxies, such as M 51 and NGC 891 imply the existence of a massive low density component (in the Taurus region, this component is directly observed through star counts). Lately, Wright et al. (1992) have reported the intensities, averaged over the whole Galaxy, of the ^{12}CO J=(1–0) through (5–4) lines, observed by COBE. These intensities, despite their low signal-to-noise ratio and the lack of ^{13}CO data, also imply the presence of two molecular components, the most massive being either extremely cold, or, which is in better agreement with the higher resolution studies, subthermally excited.

The halo model has important consequences for the constancy of the CO to H_2 conversion factor. Halos are likely to be photon-dominated regions, with A_v=0.5–1.5, where the relative abundances of H_2, ^{12}CO and ^{13}CO may vary considerably.

According to van Dishoeck and Black (1988), N(CO) may vary by factors of 3 when the UV flux increases by a mere factor of 2, and so will do W(CO) in this model. Even if, averaged over large regions (or entire galaxies) with similar global properties, $W(CO)/N(H_2)$ could stay constant, one may expect large changes when comparing intrinsically different regions such as arm and interarm regions or regions hosting active nuclei.

Some more criticisms

A discussion of further problems can be found in Maloney and Black (1988). Not only is the IS UV flux expected to vary betwen the arm and interarm regions and from the center to the periphery, but the gas 'metallicity' (i.e. the abundance of C, N, O and heavier elements, relative to H) is known to change by factors of a few from one galaxy to another. Relative to the solar system, C is underabundant by a factor of 3.3 in the LMC and a factor of 16 in the SMC (Dennefeld 1989). There is also evidence for an increase of the O/H abundance ratio from the edge to the center of several galaxies, including the Milky Way. If large, an underabundance of C or O should significantly change the value of X.

The molecular clouds may also not be gravitationally bound entities. They may be expanding/contracting, or even be stabilized by the pressure caused by an external halo, or by an internal magnetic field. In all these cases, the linewidths do not simply reflect the cloud mass.

The small scatter of the data points in Fig. 9 is surprising in this respect, all the more that the studies of nearby clouds (e.g. in the Taurus complex – Ungerechts & Thaddeus 1987) often show a much larger range of $M_{vt}/L(CO)$ ratios (e.g factors > 20). The very procedure used by Solomon and Rivolo (1987) to define the cloud boundaries in the l, b, v space could be at stake and select artificial entities, e.g. resulting from orbit crowding, which are not physically bound (Adler and Roberts 1992).

The Gas Distribution in the Galaxy according to the 'Standard' X Factor

The distribution of the gas in the Galaxy has been derived by several authors by using: i) the Berkeley and Parkes Galactic surveys of the 21-cm line emission (Weaver & Williams 1973, Kerr et al. 1986, Strong et al. 1982) and ii) the

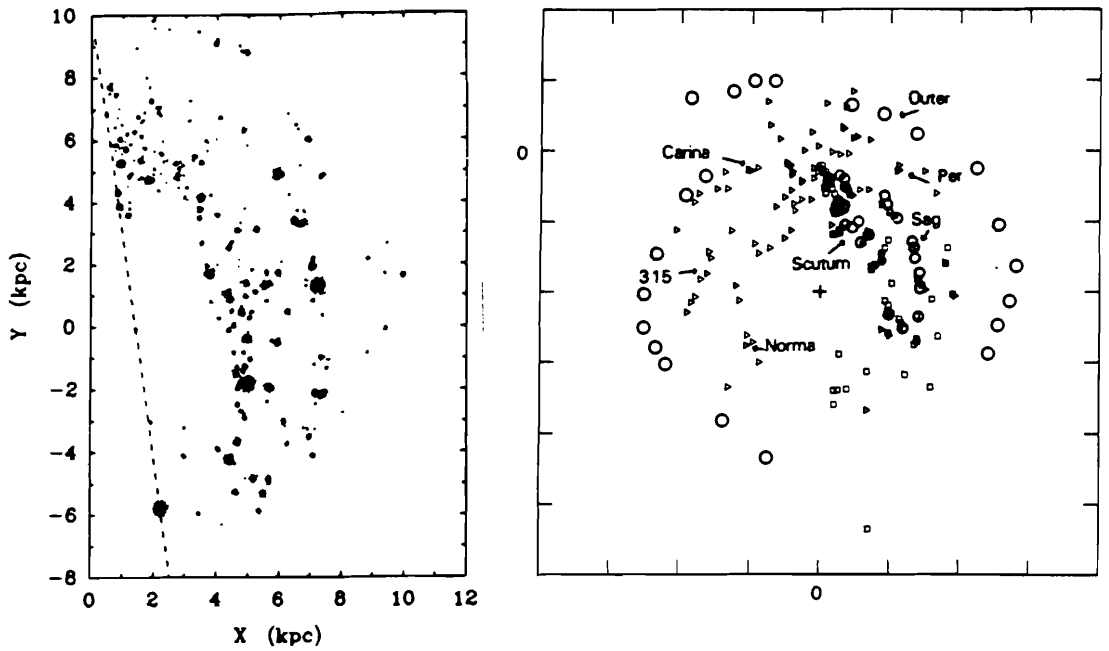

Figure 11. Face-on view of the Galactic disk, showing the location of warm molecular clouds, according to Solomon and Rivolo (1987) (*left*), as well as the relative location of the HI (*right: large open circles*), H_2 (*small open circles*), optical (*triangles*) and radio (*squares*) HII regions (from Elmegreen 1985)

Massachusetts–Stony Brook or the Columbia–Cerro Tololo surveys of the ^{12}CO(1–0) line emission (Sanders et al. 1986, Dame et al. 1987).

The 21-cm velocity-integrated line intensities are converted into N(HI) as explained above (optically thick case for low galactic latitudes) assuming that the excitation temperature is constant and equal to 125 K (see e.g. Bloemen et al. 1984). The positioning of the gas along the line of sight (and in the Galactic plane) is made by comparing the radial velocities of the main features in the observed profile to those expected from the 'standard' rotation curve.

The CO integrated line intensities are usually converted into molecular column densities $N(H_2)$ assuming a constant X factor. The Columbia and COSB groups use X= 2.3 10^{20} H_2 mol cm^{-2} K^{-1}km^{-1}s, the value derived from the diffuse γ-ray emission (Strong et al. 1988); the Stony Brook and University of Massachusets groups use X=3 (same units), a value derived from a best fit to the 'virial masses'

(Solomon & Rivolo 1987). The positioning of the CO clouds in the Galactic plane, as in the case of HI, is made according to the spectral feature velocities. Their results are summarized by Dame et al. (1987), Strong et al. (1988) and Solomon et al. (1988). The 'face-on view' of Fig. 11a, from Solomon and Rivolo (1987) shows the probable location of the brightest molecular clouds in the first Galactic quadrant and Fig. 11b, from Elmegreen (1985), a superposition of the most conspicuous molecular clouds, atomic clouds and HII regions.

Fig. 12, taken from Sanders et al. 1984, compares the average radial distributions of HI and H_2 derived in this way. Except for the nuclear region, rich is atomic and molecular gas, both distributions are ring-like, the 'molecular ring' lying well inside the HI ring. The gas is mostly molecular at galactocentric radii $R < 7$ kpc and mostly atomic further out. The HI and H_2 masses in the inner Galaxy ($R < 10$ kpc) are about equal, according to Strong et al. (1988), and close to $10^9 M_\odot$.

The X-ray interstellar flux is higher near the Galactic Center than in the vicinity of the sun. The group of Durham University (Bhat et al. 1986) reasonably argues, on the basis of the γ-ray data, that X is not constant, but decreases from 1.5 (same units) near the Sun, to 0.8 at the Galactic Center. If they are right, the HI mass inside the Solar Circle ($R < 10$ kpc) would be twice the H_2 mass. Solomon et al. (1988), because they use X=3 and the Massachusetts–Stony-Brook survey, rather than the Columbia survey, find on the opposite $M(H_2) = 2\ M(HI) = 2\ 10^9 M_\odot$.

The X Factor in Nearby Galaxies ...

Fig. 13a, from Garcia-Burillo et al. (1993) shows the CO brightness distribution in M51 observed at 1.3 mm wavelength, and Fig. 13b a superposition of the CO and 21 cm line emissions. The maps have a resolution of 12 arcsec.

The spiral structure is much more clearly visible on this figure than on Fig. 11, because M51's spiral pattern is probably more contrasted and simpler than in the Galaxy and because the Galactic picture is blurred by positioning errors.

Obviously, CO and the molecular gas are very good tracers of the inner spiral structure. The HI gas emission, which is very weak for $R < 5 - 6$ kpc (100-120"), becomes a good spiral arm tracer at larger radii. The arm-interarm contrast (W_{max}/W_{min}) is 4–6 for the CO and HI emissions.

The inner arms contain bright CO patches, which are presumably complexes of molecular clouds associated with conspicuous HII regions. These cloud complexes are marginally resolved on the high resolution interferometer maps, such as the

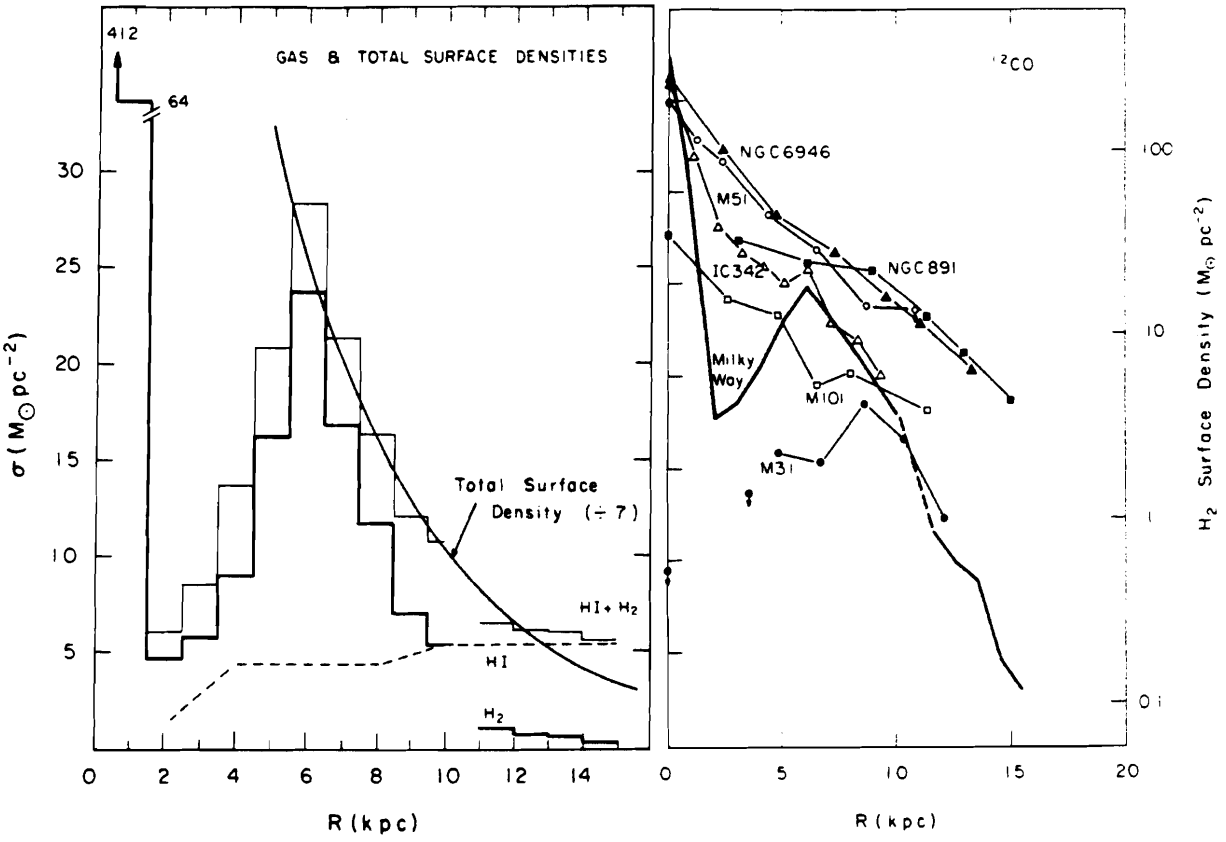

Figure 12. Comparison of the H_2, HI and total radial mass distributions in the Milky Way (*left*) and the radial distribution of H_2 in a few nearby galaxies. The H_2 column density has been derived by multiplying W(CO) by X=3.6 (standard units– from Sanders et al. 1984

OVRO and BIMA 2.6 mm line emission maps (resolution 7"; Rand and Kulkarni 1990; Adler et al. 1992).

Attempts to derive the N(H_2) to W(CO) 'conversion' factor for M51 have been made from: i) a comparison of the 'virial masses' of the CO complexes with their CO and HI 'luminosities' (i.e. W(CO) and W(HI) integrated over the cloud complex)(see: Rand and Kulkarni 1990; Adler et al. 1992); ii) comparison of the visual extinction in front of the HII regions with W(CO); and iii)derivation of the molecular gas column density by fitting the ^{12}CO and, mostly, the optically thin ^{13}CO line intensities (Garcia-Burillo et al. 1993). The results range from X= 0.8 to

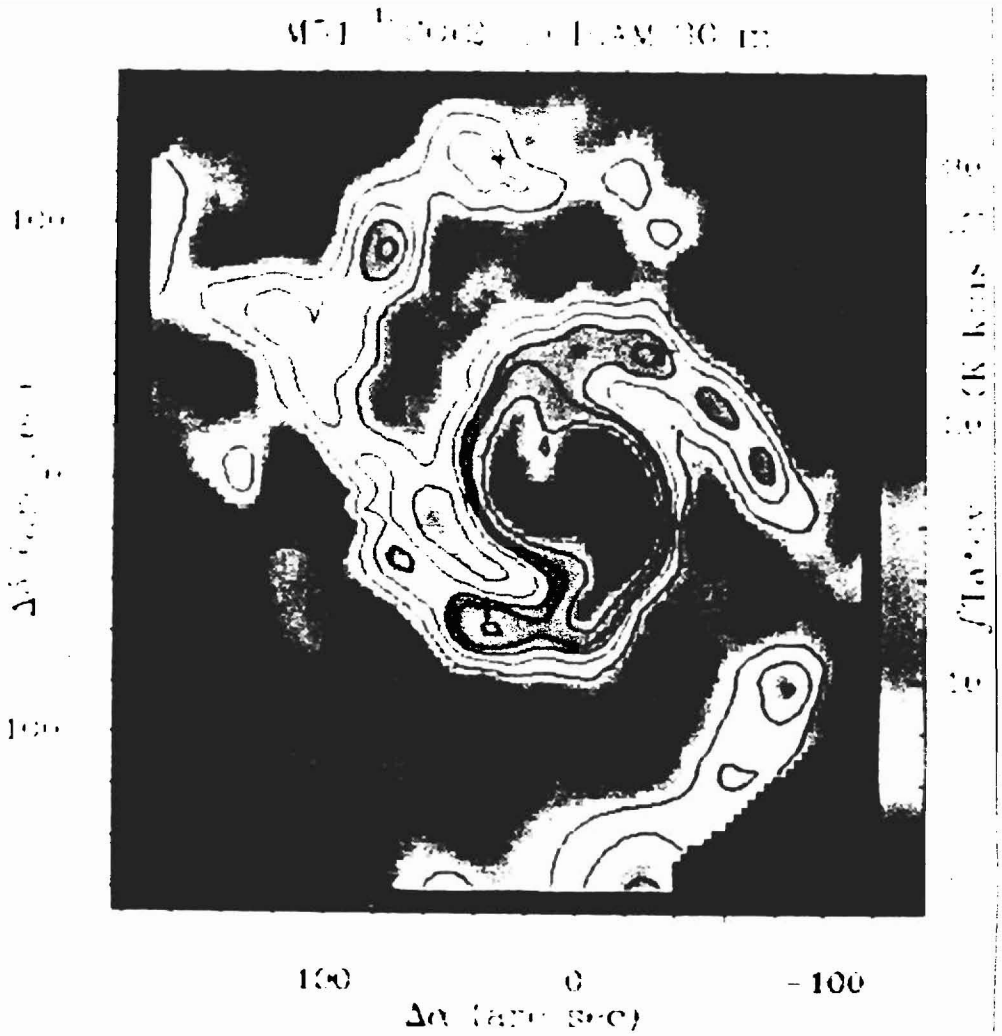

Figure 13a. The ^{12}CO velocity-integrated intensity (*contours*) in M51, observed with the IRAM 30-m telescope. Angular resolution is 12" (from Garcia-Burillo et al. 1993)

X=3 (i.e. have a reasonably small scatter) and are in rough agreement with those obtained for the Galaxy. In the case of M51, the derivation of 'virial' masses is even more problematic than in the case of the Galaxy, since the linear resolution of the observations exceed 100 pc. Note that a lower limit on the value of X in M51's arms, derived from the optically thin ^{13}CO lines, is X=0.4. Moreover, X seems to be 1–2 times smaller for the interarm gas than for the arms.

Two conclusions can be reached from the above: most of the molecular and atomic gas lies in the arms and the gas in M51 is mostly molecular.

Other nearby galaxies have been studied through the CO millimeter lines in more or less details: M31, M33, M81, NGC891, NGC6946, LMC, SMC... (a compilation up to 1989 can be found in Young 1990). The radial distribution of

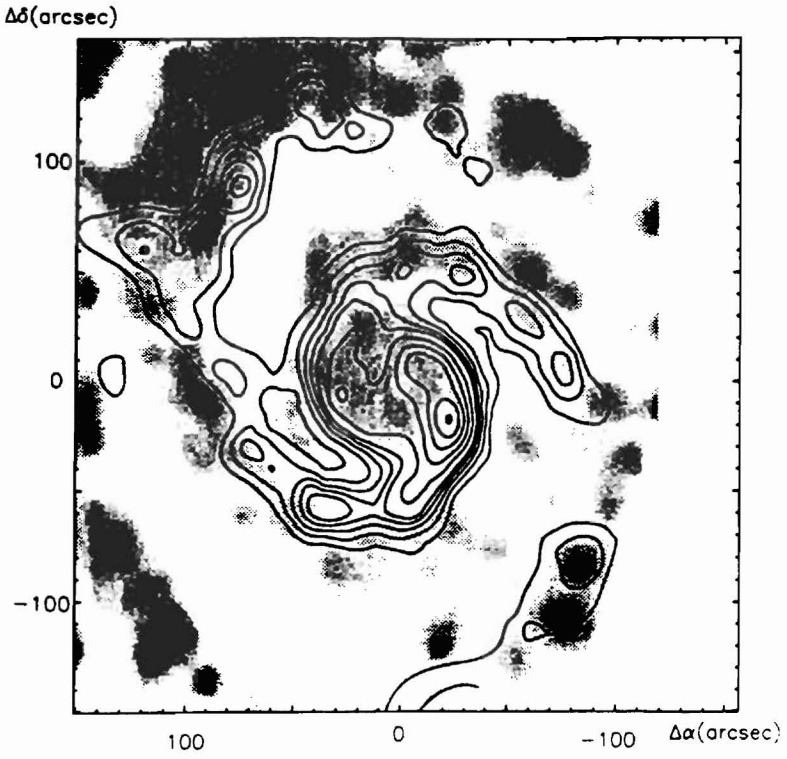

Figure 13b. The CO integrated intensity map of Fig. 13a superposed on a map of the 21 cm line emission (*grey scale*). The contours represent more or less the distribution of the molecular gas and the grey scale the distribution of the neutral atomic gas (from Garcia-Burillo et al. 1993)

W(CO) in some of them are presented in Fig. 12. M31, M33 and the Magellanic Clouds lie close enough that one can hope to resolve gravitationally bound complexes, hence be able to apply the 'virail mass' method. This has been done for M31 and M33 by Wilson et al. (1990) and for the Magellanic Clouds by Cohen et al. (1988), Rubio et al. (1990) and Johansson (1991). The latter author, who used the SEST 15-m telescope (a twin of the Bure antennas, shown on Fig. 2) benefits from a spatial resolution of ≈10 pc.

Wilson et al. (1990) find for M33 a value of X close 3 (same units), similar to that in the Galaxy (but the uncertainty is large). The results, however, are quite different for the Magellanic Clouds. There, the CO intensities are between 1.5 and 25 times weaker than expected from the linewidths!

Fig. 14, from Rubio et al. (1991), shows the linewidth–CO luminosity relations observed for the LMC, the SMC and the Galaxy, with the Cerro Tololo 1.2 m telescope. Although the differences in spatial resolution between the Galactic and extragalactic clouds and the weakness of the LMC and SMC lines may biase this plot (see e.g. the discussion of Johansson 1991), the X factor seems to be very different for the 3 galaxies.

Cohen et al. (1988) find X 6 times larger in the LMC than in the Galaxy (but Johansson 1991, from a more limited, but higher sensitivity and higher resolution survey a value of X only 1.5 times larger). Rubio et al. find X= 60 H_2 mol cm^{-2} $K^{-1}km^{-1}s$, i.e. a value 26 times larger, in the SMC. These authors interpret the larger values of X in the Magellanic Clouds as resulting from the lower metallicity and/or lower self-shielding of CO against photodissociation. It is remarkable that $C^{18}O$ seems very underabundant with respect to ^{13}CO in the LMC (Johansson 1991). This could be the signature of an enhanced photodissociation.

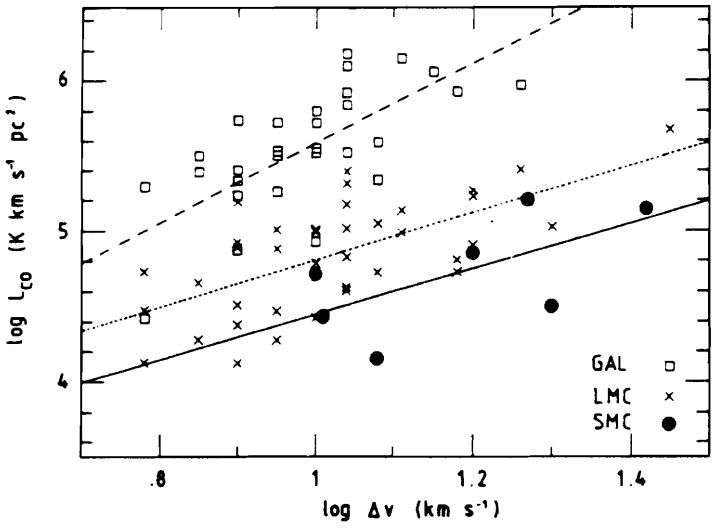

Figure 14. The linewidth–CO luminosity relations observed for the LMC, the SMC and the Galaxy (from Rubio et al. 1991)

... and in Remote Galaxies

We have seen that the far IR continuum emission can be used to trace the warm dust column density (T> 30K), provided the dust temperature is known. IRAS has provided the luminosity of a number of external galaxies in 4 far IR bands (12., 25. 60 and 100 μm). From these 4 band measurements it is possible to derive the average dust 'color' temperature, and from some assumptions about $Q_e(\lambda)$ (the dust emissivity), the 'average' dust temperature. From there, the dust column density (and the gas column density, if one assumes a constant dust-to-gas mass ratio) can be estimated (this assumes that the actual dust temperature is not very different from the 'average' value).

This method has been applied by several authors to estimate the gas mass independantly of the CO + HI method described above. Of course, the FIR method is very crude as it is insensitive to the cold dust, whose emission is observable only at much lower wavelengths (e.g. 0.8 mm).

As illustarted in Fig. 15a (from Sanders et al. 1987), there is a good correlation between the total far IR luminosity and the CO luminosity for the bright IRAS galaxies. 'Quiet' galaxies such as the Milky Way, M51 and M101 lie along the line $L_{fir}/L_{CO} = 23L_{\odot}$. Starburst galaxies have L_{fir}/L_{CO} ratios of 70–100 $L_{\odot}$ and lie on the left of the line. Finally, the most luminous objects the 'active galactic nuclei' (AGNs), such as Mrk 231, have even greater L_{fir}/L_{CO} ratios and lie in the upper right corner of the figure. Obviously, these different types of galaxies have different dust temperatures and, my be, grain properties.

Devereux and Young (1990) have attempted to account for the differences in dust temperature, the latter being derived from the I_{100}/I_{60} 100μm to 60μm IRAS flux ratio, assuming $Q_e \propto 1/\lambda$. The result is shown in Fig. 15b for inner part of the bright spiral galaxies. The estimated dust mass is plotted in abscissa and the HI+H_2 mass in ordinate. (the HI mass is derived from 21 cm line measurements and the H_2 mass from 2.6 mm CO measurements, using X=2.8 in the above units.) In some spirals (open circles), the H_2 mass is larger than the HI mass, in other (black dots), the HI mass dominates.

Devereux and Young interpret the small dispersion in the graph by the existence of a single value of X for all spirals (within 30% equal to 2.8). Their view, however, is probably too optimistic, as a good correlation between the dust and CO emissions does not mean that these quantities trace H_2 (they could reflect, for example, the 'metal' abundance). More interesting is the fact that the galaxies brighter in HI than in CO (black dots), for which the gas mass is more accurately measured,

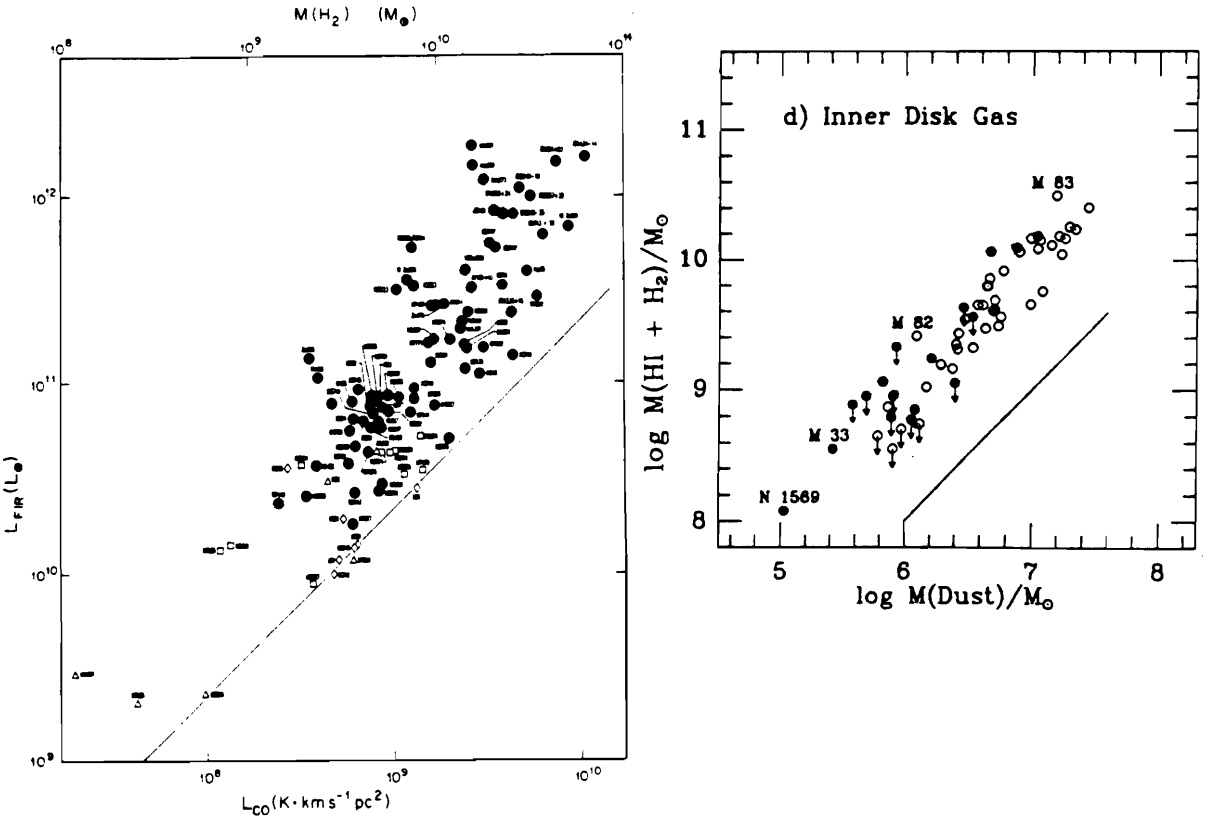

Figure 15. **15a**(left): The FIR luminosity determined from IRAS 60-100μm data, versus the CO luminosity, for the bright IRAS galaxies. The diagonal line corresponds to L_{fir}/L_{CO}= 23 and goes through the Milky Way data point (from Sanders et al. 1987). **15a**(right): The total gas mass versus the dust mass for the IR bright spirals (from Devereux and Young 1990)

follow the same relation as the other spirals. This could mean that the dust masses in Fig. 15 are properly determined and that the gas-to-dust mass ratio, indeed, is about constant. The small number of HI-dominated spirals and the large number of upper limits in the graph (which show that the lower border of the data point cloud is largely instrumental) could well have mask a much larger scatter of X values.

Evidence that the 'standard' Galactic X factor does not apply to the ultra-luminous galaxies, comes from the very large H_2 masses, relative to stellar masses, derived for some systems: Wang et al. (1991) find for the inner part of NGC 6240, an apparently edge-on interacting galaxy, an H_2 mass > 3 times larger than the stellar mas. (A lower limit to the total stellar+gas mass is derived from the CO linewidth,

by assuming a radius of 1.5 kpc and a spherical mass distribution). As pointed out above, the H_2 mass of the primeval galaxy IRAS10214, derived from the standard Galactic X factor, is about 1/2 the total mass of the Milky Way, which is uncon-fortably large in view of the relatively narrow CO linewidth (400 kms^{-1}). Clearly before seing in these numbers a result of galactic evolution, one has to consider the derived H_2 masses with great caution.

Conclusion

Although it certainly varies by large factors from place to place (e.g. between the cloud cores and halos), the CO 'standard' conversion factor, $X = N(H_2)/W(^{12}CO$ 1-0)$= 2.3$ H_2 mol cm^{-2} $K^{-1}km^{-1}s$, seems to apply globally to the Milky Way and the nearby spirals with an uncertainty of a factor of 3 or so. In the other systems, such as the irregular and elliptical galaxies and in the AGNs, X is probably variable and much more uncertain.

REFERENCES

Adler et al. 1992, Ap. J. 392, 497

Bernes, C. 1979, A&A 73, 67

Bhat, C.L. et al. 1986, Phil. Trans. Roy. Soc. 319, 249.

Bohlin et al. 1978, Ap. J. 224, 132

Bloemen et al. 1984, A&A 139, 37

Bloemen, J.B.G.M. et al. 1986, A&A 154, 25.

Brown, R.L. and Vanden Bout, P.A. 1991, A.J. 102, 1956

Cohen, R.S. et al. 1988, Ap.J. 331, L95

Cox, P. and Mezger, P.G. 1983, A&A Review 1, 49

Dame et al. 1987, Ap. J. 302, 706

Dennefeld, M. 1989, in "Recent Dev. of Magellanic Cloud Research", eds. de Boer et al. p. 107, Observatoire de Paris

Devereux, N.A. and Young, J.S. 1990, Ap. J. 359, 42

Dickman, R.L. et al. 1986, Ap. J. 309, 326.

Elmegreen, D.M. 1985, in "The Milky Way Galaxy", I.A.U. Symp. 106, p. 255, eds. H. van Woerden et al. Reidel Publ.

Garcia-Burillo, S., Guelin M., Cernicharo, J. 1993, A&A in press

Goldreich, P. and Kwan, J. 1974, Ap. J. 189, 441

Guélin, M. and Cernicharo, J. 1987, in "Molecular clouds in the Milky Way and external galaxies", ed. Dickman et al. , Reidel

Guélin, M. and Cernicharo, J. 1988, in "The physics and chemistry of interstellar molecular clouds", ed G. Winnewisser and J.T. Armstrong, Springer

Guilloteau et al. 1992, A&A 262, 624

Herzberg, G. 1950, in "Spectra of Diatomic Molecules" p. 340, van Nostrand Reinhold

Hildebrand, R. H. 1983, Q. Jl. R.A.S. 24, 267

Johansson, L.E.B. 1991, Proc. I.A.U. Symp. 146, eds Combes & Casoli, Kluwer Acad. Publ.

Kerr et al. 1986, A&A Suppl. 66, 373
Letzelter, C. et al. 1987, Chem. Phys. 114, 273
Liszt, H. 1982, Ap. J. 262, 198
MacLaren, I. et al. 1988, Ap. J. 333, 821
Maloney, P. and Black, J.H. 1988, Ap. J. 325, 389
Mezger, P.G. et al. 1990, Proc. IAU Symp. 147, p.245
Rowan-Robinson, M. et al. 1991, Nature 351, 719
Rubio, M. et al. 1991, Ap. J. 368, 173
Rand R.J. and Kulkarni, S.R. 1990, Ap. J. 349, L43
Sanders et al. 1984, Ap. J. 276, 182
Sanders et al. 1986, Ap. J. Suppl. 60, 1
Sanders et al. 1987, in "Molecular clouds in the Milky Way and external galaxies", ed. Dickman et al. , Reidel
Spitzer, Lyman, Jr. "Physical Processes in the IS Medium". J. Wiley & Sons 1978 pp. 42-44, 70-87, 122-129, 149-164.
Solomon, P.,M., Rivolo, A.R. 1987, in "The Galaxy", eds. G. Gilmore and B. Carswell, p. 105, D. Reidel Pub.
Solomon et al. 1987, Ap. J. 319, 730
Solomon, P. M. and Barrett, J.W. 1991, Proc. IAU Symp. 146, ed. Combes, F. and Casoli, F., Kluwer, p.235.
Strong et al. 1982, M.N.R.A.S. 201, 495
Ungerechts, H. and Thaddeus, P. 1987, Ap. J. (Suppl.) 63, 645
van Dishoeck, E.F. and Black, J.H. 1987, in Physical processes in interstellar clouds , ed G. Morfill, Reidel
van Dishoeck, E.F. and Black, J.H. 1988, Ap. J. 334, 771
Verter, F. 1991, Ap. J. 375, 95
Viala, Y. et al. 1988, A&A 193, 265
Wang, Z. et al. 1991, Ap. J. 368, 112
Watson, W.D. 1975, in "Les Houches- session XXVI "Physique Atomique et Moleculaire et Matiere Interstellaire", eds. Balian et al., p. 176, North-Holland Publ.
Weaver, H.,F., Williams, D.R.W. 1973, A&A Suppl. 8, 1
Wilson & Scoville 1990, Ap. J. 363, 435
Young, J.S. 1990, in "The Interstellar Medium in Galaxies", eds. Thronson & Sull, p.67, Kluwer Acad. Publ.